Joachim Höpfner

Interannual variations in length of day and atmospheric angular momentum with respect to ENSO cycles

Paper presented at the 22nd General Assembly
International Union of Geodesy and Geophysics
Birmingham, UK, 18-30 July 1999

Scientific Technical Report STR99/07

Publication: Scientific Technical Report
No.: STR99/07

Interannual variations in length of day and atmospheric angular momentum with respect to ENSO cycles

Joachim Höpfner

GeoForschungsZentrum Potsdam, Division 1: Kinematics and Dynamics of the Earth,Telegrafenberg, D-14473 Potsdam, Germany; E-mail: ho@gfz-potsdam.de

Abstract. At interannual time scales, the excitation of variations in Length-Of-Day (LOD) is caused by two prominent signals in the atmosphere: The El Niño-Southern Oscillation (ENSO) and the Quasi-Biennial Oscillation (QBO). The axial Atmospheric-Angular-Momentum (AAM) component χ_3 is related to changes in LOD. Focussing on the interannual variations in the solid Earth-atmosphere axial angular momentum budget, we consider the Low-Frequency Component and the Quasi-Biennial Oscillation in LOD and AAM in their temporal variability. In particular, we use the time series of LOD data of the series EOP (IERS) 97C04 from 1962 to 1998 and of χ_3 data of the series AAM (NCEP) Reanalysis from 1958 to 1998, AAM (JMA) from 1983 to 1998, AAM (ECMWF) from 1988 to 1996, and AAM (UKMO) from 1986 to 1998. To separate the interannual signals, we apply low-pass and band-pass filters. For comparison, the monthly data of the Southern Oscillation Index (SOI), as given by the NOAA as the difference in the surface pressure between Tahiti and Darwin, Australia, are processed and exhibited in the same manner. The main results are quantitative estimates of the Low-Frequency Component and the Quasi-Biennial Oscillation in the LOD, AAM and SOI variations and of the total interannual signals in the AAM and SOI variations. Also, the decadal LOD component is available as a function of time.

Key words: AAM (atmospheric angular momentum), Earth's rotation, LOD (length of day), interannual variations, ENSO (El Niño-Southern Oscillation), QBO (Quasi-Biennial Oscillation), SOI (Southern Oscillation Index).

1 Introduction

With regard to the conservation of the total angular momentum of the entire Earth, variations of Earth rotation, measured by changes in the Length-Of-Day (LOD), and polar motion (PM) reflect the exchange of angular momentum between the solid Earth, atmosphere, ocean, hydrosphere, and other geophysical fluids. Changes in the angular momentum of a component of the Earth result from redistributions of its mass and from changes in the strength of its motion fields. In these geophysical processes, it is the atmosphere that plays the dominant role on interannual, seasonal and intraseasonal time scales. Seasonal oscillations in LOD are the largest signals that are of atmospheric origin. Also, fluctuations at interannual time scales are important components, including the El Niño-Southern Oscillation (ENSO) and the Quasi-Biennial Oscillation (QBO).

Effective Atmospheric-Angular-Momentum (AAM) functions related to the Earth rotation as described by Barnes et al. (1983) are used to compute numerically AAM time series by the world's meteorological centers. Here, the equatorial components χ_1 and χ_2 are associated with the excitation of PM, and the axial component χ_3 is related to changes in LOD.

Our previous studies based on LOD and χ_3 data sets were concerned with the imbalances in the solid Earth-atmosphere axial angular momentum budget at seasonal time scales (Höpfner, 1996, 1997, 1998a, b). In this study, we focus on the interannual variations in LOD and AAM, which can lead to a better understanding of the global atmospheric cycle. It is appropriate to describe the relationship between changes in LOD and AAM (Section 2) and to give general characteristics of interannual signals (Section 3) before discussing the data sets used (Section 4), data processing (Section 5) and results (Section 6). Section 7 gives a summary and some concluding remarks.

2 Relationship between changes in LOD and AAM

The time of the Earth clock denoted by Universal time (UT1) is expressed as the differences with the atomic time scale (Temps Atomique International, abbr. TAI), and the observed period of rotation of the Earth is the day. LOD is the excess of the duration of the day relative to the standard length, which is 86400 s.

For changes in LOD that are caused by geophysical processes, its relationship to the excitation function ψ has the form

$$LOD = \psi_3 + constant, \tag{1}$$

where ψ_3 is the axial component of ψ.

If the solid Earth and the atmosphere form a closed dynamical system, then changes in AAM about the polar axis relative to an Earth-fixed frame must be reflected by compensating changes in the Earth's axial angular momentum. Therefore, the expression is as follows:

$$LOD_{atm} = -\chi_3. \tag{2}$$

Here, LOD_{atm} is the atmospheric contribution to LOD inferred from AAM.

Concerning the effective AAM functions (Barnes et al., 1983), the components χ_1, χ_2 and χ_3 can be partitioned into contributions by wind and pressure. As noted above, we are here only concerned with the axial component χ_3, in particular with the wind term labelled χ_3(W), and with the pressure term without and with Inverted-Barometer (IB) response labelled χ_3(P) and χ_3(P+IB), respectively. Compared to χ_3(W), the pressure term χ_3(P) or χ_3(P+IB) represents only a small contribution to the total χ_3 component.

The AAM data are non-dimensional, while LOD data are given in units of seconds of time (s). Thus, the AAM data are converted into LOD_{atm} values by inverting their signs and multiplying them with the scale factor of 86 400. For additional details, see, e. g., Höpfner (1998b) and references therein.

3 General characteristics of interannual variations

In view of the necessity of weather predictions, the atmosphere is currently the best measured fluid of the Earth's subsystems, i. e., atmosphere, hydrosphere including the oceans, cryosphere, lithosphere and biosphere. In particular, the past two decades have seen remarkable advances in our understanding of the general circulation of the atmosphere. This progress was achieved because of breakthroughs in measurements of the relevant atmospheric parameters. In the Earth's climate system, the atmosphere is characterized by a broad spectrum of processes with temporal variability. The brief review here is restricted to the interannual variations. As mentioned above, there are the El Niño-Southern Oscillation and the Quasi-Biennial Oscillation. On interannual time scales, fluctuations in the AAM and LOD are attributed to these large-scale circulation changes.

Interannual variations predominantly arise from interactions of the combined atmosphere-ocean system with many positive and negative feedbacks; see Peixoto and Oort (1992). As the name suggests, the phenomenon of the El Niño-Southern Oscillation (ENSO) consists of two components: El Niño as the mainly oceanic component and Southern Oscillation as the mainly atmospheric component.

Historically, El Niño (that is the Spanish name for the Christ child) has been associated with a weak, warm current. Replacing the usually cold waters of the Peru current, it appears along the coast of Ecuador and Peru annually around Christmas time. Today, the name refers to a larger-scale phenomenon occurring every three to seven years. During the event, the normally cold waters over the entire eastern equatorial Pacific Ocean show a dramatic warming of several degrees. Moreover, there are very large anomalies in the oceanic and atmospheric circulations and in the global weather. The Southern Oscillation that occurs in conjunction with these anomalies is manifested by large east-west shifts of mass in the tropical atmosphere between the Indian and West Pacific Oceans and the East Pacific Ocean.

Concerning the principal atmosphere-ocean interactions, it is worth remarking that the ocean influences the atmosphere mainly through anomalies in the sea-surface temperatures, while the atmosphere influences the oceans mainly through anomalies in the surface wind stress. Thus, a complicated coupled system exists, i.e., the sea-surface temperature anomalies produce anomalies in the surface winds and in the general circulation of the atmosphere, and the anomalies in the surface wind stress in turn produce anomalies in the circulation of the ocean and, eventually, in the sea surface temperatures.

Also, there are significant east-west circulations in the equatorial atmosphere for normal, non-ENSO conditions. Here, westward trade winds over the central equatorial Pacific Ocean maintain a difference in the sea level of about 40 cm between the east and west coasts. For some reason, departures from normal for so-called Walker circulation are the following:

(a) If the trade winds weaken, this is associated with warmer than normal sea-surfaces temperatures in the eastern equatorial Pacific, which leads to El Niño, i. e., ENSO conditions;

(b) if the trade winds strengthen, this is associated with cooler than normal sea-surface temperatures in the eastern equatorial Pacific, which leads to anti-El Niño or La Niña, i. e., anti-ENSO conditions.

In the early stages of an ENSO episode, the surface pressure decreases over almost the entire eastern Pacific Ocean and increases over the western Pacific and Indian Oceans. Stations near the maximum and minimum values of the sea-level pressure are Darwin, Australia (12^oS, 131^oE) and Tahiti (17^oS, 149^oW), respectively. During ENSO (anti-ENSO) conditions, there is relative high (low) pressure at Darwin, but relative low (high) pressure at Tahiti. The Southern Oscillation Index (SOI) is computed as the difference in the sea-level pressure between both stations. If this index is a small negative number (a large positive number), then an ENSO (anti-ENSO or La Niña) event is in progress.

The Quasi-Biennial Oscillation (QBO) occurs in the tropical troposphere and stratosphere. It can be found in the zonal winds and temperature with an irregular period of about two years. Especially in the zonal winds, the QBO signal shows a pattern of alternating westerly and easterly winds over the equator. Probably, it results from wave-mean flow interactions in the atmosphere. Solar-QBO-climate connections are possible in modulating solar effects on the atmosphere by the quasi-biennial cycle. For more details on the interannual variations in the Earth's climate system, see Peixoto and Oort (1992) and references therein.

As mentioned above, interannual variations are present in the axial AAM, and they, in turn, are associated with corresponding changes in LOD. During the last decade, significant improvements in atmospheric and geodetic data sets have enabled studies of these signals on all time scales. See Dickey (1990), Hide and Dickey (1991) and Rosen (1993) for overviews of advances in this field.

Interannual fluctuations in AAM and LOD have been studied by Chao (1984, 1988) and Eubanks et al. (1986), who have shown that ENSO has a significant influence on LOD changes at interannual time scales. Salstein and Rosen (1986) demonstrated a connection between El Niño events and LOD changes using a historical record of LOD fluctuations from 1860 to present. Chao (1989) investigated the combined effect of ENSO and QBO on interannual LOD variations. Using data from 1964 to 1987, his correlation studies indicated that the interannual atmospheric contribution to axial angular momentum accounts for most of the observed interannual LOD variation. Dickey, Marcus and Hide (1992) reported on global-scale propagation of AAM fluctuations originating in equatorial regions on interannual time scales from 1976 to 1991. Using SOI records, the interaction between the low-frequency and quasi-biennial components is demonstrated to result in different climatic events such as strong El Niño and related La Niña. Dickey et al. (1994) performed a case study of the Earth's interannual momentum budget during the unusually strong and well-observed 1982-1983 ENSO.

Chao and Naito (1995) showed the time-frequency characteristics of LOD and AAM changes by wavelet spectra. This allowed them to demonstrate the time evolution of the oscillatory patterns of the ENSO and QBO components. Gross et al. (1996) reported that SOI and changes in amplitude of the seasonal LOD signals correlate. This fact demonstrates a linkage between seasonal LOD variability and, therefore, between seasonal zonal wind variability and the ENSO phenomenon in the climate system. For the influence of ENSO on correlations between seasonal and subseasonal variations of Earth rotation and AAM, see also Nuzhdina, Kołaczek and Kosek (1997). Salstein and Rosen (1998) determined interannual, seasonal and intraseasonal bands in AAM from a 40-year reanalysis. They showed that strong AAM anomalies related to El Niño-Southern Oscillation exist throughout the record. Also, Quasi-Biennial Oscillations are present in the reanalysis series of the AAM data incorporating higher stratospheric levels up to 10 hPa. To represent ENSO and QBO that are local in time and frequency we apply digital filters as in studying the solid Earth-atmosphere axial angular momentum balance at seasonal frequencies (Höpfner, 1996, 1997, 1998a, b).

4 Data sets used in this study

To investigate the variations in LOD and AAM at the interannual time scale, the following series of data at one-day intervals are used:

(a) LOD of the series EOP (IERS) 97C04 computed as a combined solution by the International Earth Rotation Service (IERS) and

(b) χ_3 of the series AAM (NCEP) Reanalysis, AAM (JMA), AAM (ECMWF) and AAM (UKMO).

Here, NCEP stands for U. S. National Centers for Environmental Prediction, JMA for Japan Meteorological Agency, ECMWF for European Centre for Medium-Range Weather Forecasting and UKMO for U. K. Meteorological Office.

Table 1 summarizes the LOD and AAM data and the associated time intervals in calendar days and in Modified Julian Date (MJD). All time series are available to the year 1998, but the AAM (ECMWF) series has a 10-month gap.

For information on the series EOP (IERS) 97C04, see the 1997 IERS Annual Report (IERS, 1998). The LOD data include oscillations due to zonal tides for periods under 35 days in full size. By adopting IERS Conventions

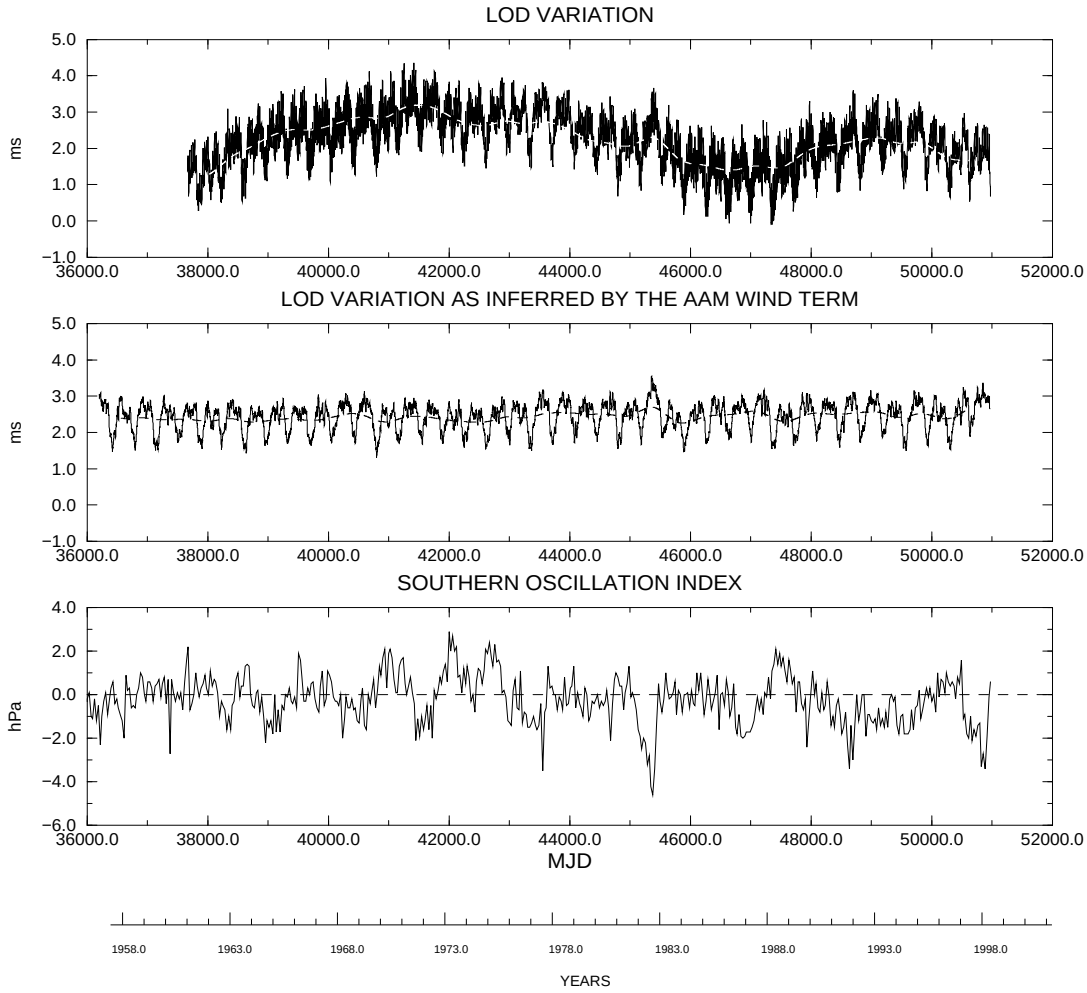

Figure 1. LOD and LOD_{atm} variations and the SOI time series. Top: LOD variation as computed by IERS. Centre: LOD_{atm} variation as inferred by the axial component of AAM computed by NCEP Reanalysis, in particular by the wind term χ_3(W) with 10 hPa level. The Low-Frequency Components of the LOD and LOD_{atm} variations are shown as dashed lines. Bottom: Southern Oscillation Index (SOI) time series, i. e., the monthly differences in sea level pressure between Tahiti and Darwin, Australia, as computed and standardized by NOAA.

Table 1. LOD and AAM data used. MJD is the Modified Julian Date.

Time series	Time interval (calendar days)	Time interval (MJD)
EOP (IERS) 97C04	Jan. 1, 1962 ... June 15, 1998	37665.0 ... 50979.0
AAM (NCEP) Reanalysis	Jan. 1, 1958 ... May 31, 1998	36204.0 ... 50964.0
AAM (JMA)	Sept. 28, 1983 ... Feb. 6, 1998	45605.0 ... 50850.0
AAM (ECMWF)	Jan. 1, 1988 ... June 30, 1996	47161.0 ... 50264.0
	Apr. 30, 1997 ... Feb. 7, 1998	50568.0 ... 50851.0
AAM (UKMO)	Nov. 27, 1986 ... Feb. 7, 1998	46761.0 ... 50851.0

(McCarthy, 1996), the tidal contribution is removed from the LOD data. Therefore, after reduction of the tidal oscillations, the data are designated by LOD_{red}.

The AAM time series are obtained from the Special Bureau for the Atmosphere (SBA), formerly IERS Sub-Bureau for AAM (Salstein et al., 1993). Note that the series AAM (NCEP) Reanalysis has the longest time interval and is based on the NCEP/NCAR reanalysis products, where NCAR is the acronym for U. S. National Center for Atmospheric Research. For details concerning these reanalyses, see Kalnay et al. (1996). Information on the angular momentum calculations from the reanalysis can be found in Salstein and Rosen (1997). Some comment on the wind terms χ_3(W) of AAM is appropriate here: χ_3(W) is computed by volume integrals of wind fields. For the four meteorological centers, the pressure levels over the depth of the atmosphere in the global circulation models (GCM) are different. Especially, the top pressure levels are 10 hPa for NCEP Reanalysis, JMA and ECMWF, but about 25 hPa for UKMO. Compared with the AAM (NCEP) reanalysis data, the AAM (JMA), AAM (ECMWF) and AAM (UKMO) series are produced operationally and therefore not free of gaps and discontinuities caused by procedural changes over the entire time intervals. The preprocessing of the operational series is completed and carried out, respectively, as described by Höpfner (1997, 1998b).

Figure 1 shows the variations of LOD and LOD_{atm}. We can see the changes in LOD as computed by IERS at the top and those in LOD_{atm} as inferred from AAM for the wind term χ_3(W) computed by NCEP Reanalysis at the centre. Each curve is shown together with its Low-Frequency Component obtained by low-pass filtering. For information about this, see Section 5. Some important points are the following: Generally, there is a rich variability over a wide range of time scales. However, compared to the LOD time series, those of LOD_{atm}, especially for the χ_3(W) terms, show no significant long-term component. Probably, the decadal signal in LOD is the result of a core-mantle angular momentum exchange; see, e. g., Jochmann and Greiner-Mai (1996). Further representations of the LOD and LOD_{atm} time series can be found in Höpfner (1997, 1998a, b).

For purposes of comparison, a record of the Southern Oscillation Index (SOI) as measure of the large-scale fluctuations in sea level pressure occurring between the western and eastern tropical Pacific during the El Niño-Southern Oscillation cycles may be processed in the same manner. The monthly time series of the SOI computed as differences in sea level pressure anomaly between Tahiti and Darwin, Australia, is routinely available from the National Oceanic and Atmospheric Administration (NOAA). Also plotted in Fig. 1, at the bottom, are the standardized SOI data from 1957 to 1998 used in this study. Here, it is worth remarking that the generally accepted El Niño events occur in the following years: 1957, 1963, 1965, 1969, 1972, 1976/77, 1982/83, 1986/87, 1991-1993, 1994/95, and 1997/98.

5 Data processing

5.1 LOD_{red} and LOD_{atm} time series

To study the behaviour of the interannual signals as a function of time, the time series of LOD_{red} and LOD_{atm} are separately processed with respect to the Low-Frequency Component and the Quasi-Biennial Oscillation by using digital filters. For comparison, the characteristics of the digital filters used here and in our previous studies (Höpfner, 1996, 1997, 1998a, b) are given in Table 2. To exhibit that the different components are well separated from each other by using the filters, Fig. 2 displays the amplitude characteristics of the filters. These are computed as the response function for each filter in terms of the ratio of the amplitude of the fluctuations after filtering to that before.

For the time intervals of the resulting series of the Low-Frequency Component and the Quasi-Biennial Oscillation filtered out from the original LOD_{red} and LOD_{atm} series, see Table 3. Important aspects of the data processing are the following:

(a) Low-Frequency Component

As in our previous studies (Höpfner, 1996, 1997, 1998a, b), the Long-Frequency Components are separated by low-pass filtering the data at one-day intervals. The filter procedure designed by Höpfner (1996) is again applied to isolate the

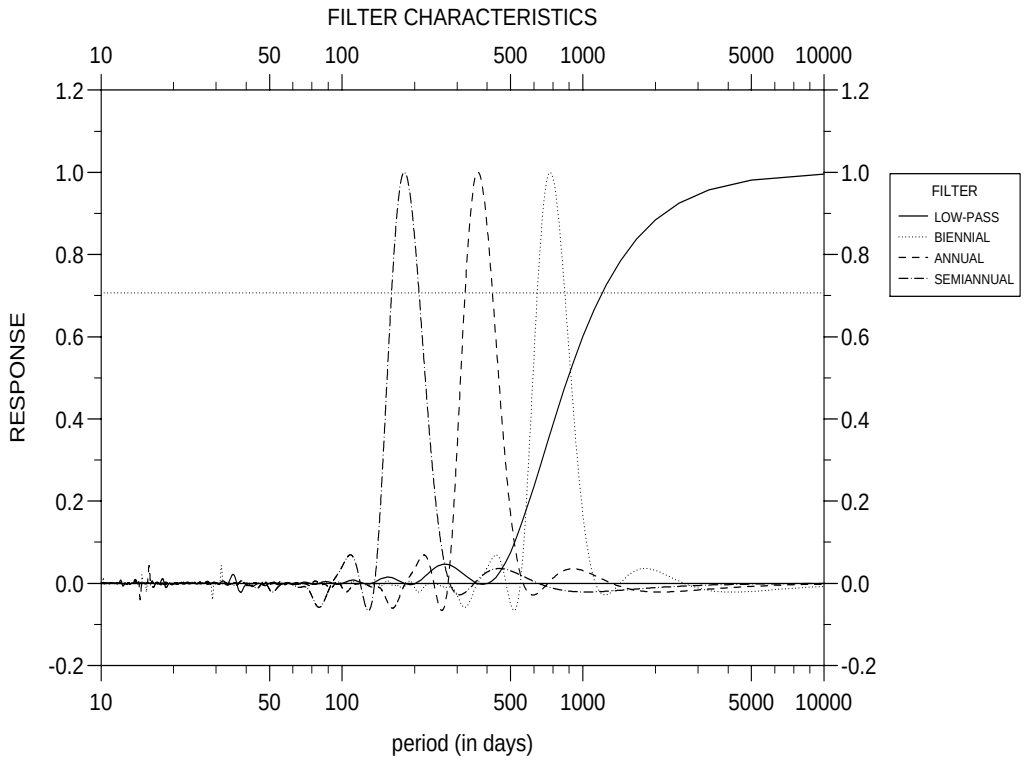

Figure 2. Amplitude characteristics of the filters applied for separating the long-term component and the biennial, annual and semiannual oscillations from the original time series. The response is given as function of period. Half-power points are the points of intersection between the individual curves and the horizontal light dotted line.

Table 2. Characteristics of the digital filters used for one-day sampling.

Filter: Component	Number of points used in each filtering	Related edge effect: Points lost at either end	(a) Cut-off period of the low-pass filter (b) Half-power points of the filter (days)
Low-pass: Low-Frequency	731	365	(a) 415 (b) 1206
Band-pass: Biennial	3171	1585	(b) 648 and 840
Annual	1589	794	(b) 324 and 421
Semiannual	787	393	(b) 160 and 208

Low-Frequency Components from the LOD_{red} time series and the different LOD_{atm} time series.

(b) Quasi-Biennial Oscillation

To filter out a biennial oscillation from daily values of time series, a zero-phase digital band-pass filter is designed analogous to the band-pass filters developed for separating annual and semiannual oscillations; see Höpfner (1996, 1997, 1998a, b). The biennial band-pass filter is applied to the original LOD_{red} time series to isolate the Quasi-Biennial Oscillation in the IERS system. In the same manner as the LOD_{red} time series, the LOD_{atm} time series in the NCEP Reanalysis, JMA and UKMO systems, respectively, any of them including the wind term χ_3(W), the pressure term χ_3(P) and, if computed, the pressure IB term χ_3(P+IB) data, are band-pass filtered. Since, as noted, there is a data gap of 10 months in the LOD_{atm} time series of the ECMWF, no QBO component could be separated from these time series.

For separating the Quasi-Biennial Oscillation, it is also possible to filter out this component after the low-frequency and seasonal signals are removed from the time series. The QBO component of LOD_{red} in the IERS system and of LOD_{atm} in the NCEP Reanalysis system is computed also in this manner for purposes of comparison. Here, we use two biennial filters, the one used for filtering out the component from the original data and a biennial filter of a broader bandwidth designed for separating the component from the data after removing the low-frequency and seasonal signals. Compared to each other, the filters have a cosine shape modified over four and two periods, respectively, as weight function.

Using a simple method based on the maximum, zero crossing and minimum of a periodic function as described by Höpfner (1997, 1998b), optimal estimates of the amplitude and period of the Quasi-Biennial Oscillation filtered out from the LOD_{red} and LOD_{atm} series, including the standard deviations of the estimates, are computed.

5.2 SOI time series

To process the monthly time series of the Southern Oscillation Index with respect to the Low-Frequency Component and the Quasi-Biennial Oscillation in an analogous way to the LOD_{red} and LOD_{atm} time series at one-day intervals, corresponding digital filters are used. For this purpose, we design zero-phase digital low-pass and biennial filters for separating these components from monthly values. Also, the calculation of optimal estimates of the amplitude and period of the QBO component of SOI and their standard errors is made in the same manner as for the LOD_{red} and LOD_{atm} results.

Table 3. Time intervals for the Low-Frequency Component and the Quasi-Biennial Oscillation filtered out from the original LOD_{red} and LOD_{atm} series given in calendar days and MJD.

Time series: Center / System	Low-Frequency Component	Quasi-Biennial Oscillation
LOD_{red}: IERS	Jan. 1, 1963 ... June 15, 1997 38030.0 ... 50614.0	May 5, 1966 ... Febr. 11, 1994 39250.0 ... 49394.0
LOD_{atm}: NCEP Reanalysis	Jan. 1, 1959 ... May 31, 1997 36569.0 ... 50599.0	May 5, 1962 ... Jan. 27, 1994 37789.0 ... 49379.0
JMA	Sept. 27, 1984 ... Feb. 6, 1997 45970.0 ... 50485.0	Jan. 30, 1988 ... Oct. 5, 1993 47190.0 ... 49265.0
ECMWF	Dec. 31, 1988 ... July 1, 1995 47526.0 ... 49899.0	
UKMO	Nov. 27, 1987 ... Feb. 7, 1997 47126.0 ... 50486.0	March 31, 1991 ... Oct. 6,1993 48346.0 ... 49266.0

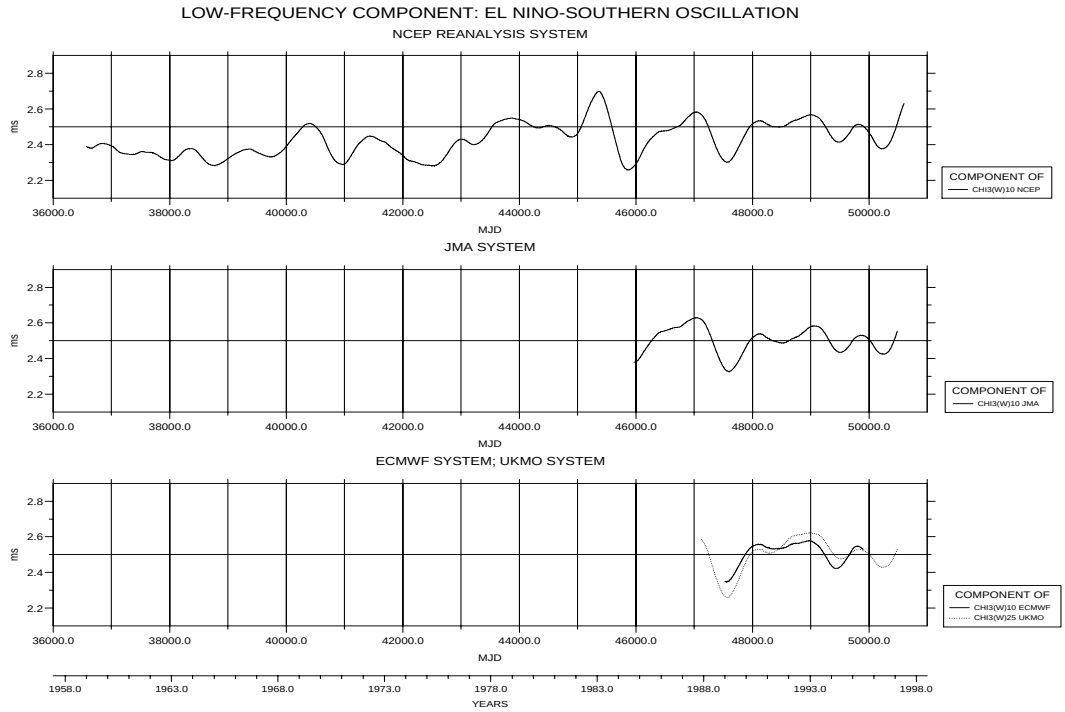

Figure 3. Low-Frequency Components in the LOD_{atm} variations for the different systems: Component of the wind term χ_3(W) in the NCEP Reanalysis system (top), in the JMA system (centre), and in the ECMWF and UKMO systems (bottom). The number added to each χ_3(W) gives the upper pressure level in the atmosphere in hPa used in computing the values.

6 Discussion of the results

Before describing and assessing the results obtained for the interannual band, the following discussion of the results serves to distinguish between the Low-Frequency Component and the Quasi-Biennial Oscillation relating to the different systems:

(a) Low-Frequency Component

Figure 3 shows the Low-Frequency Components of the LOD_{atm} series in terms of the wind term χ_3(W) in the different systems. The curve for the NCEP Reanalysis system is displayed in the top panel, that in the JMA system for the middle panel and the curves for the ECMWF and UKMO systems in the bottom panel. Note that the number added to each χ_3(W) in this and following figures gives the pressure at the top level of the atmosphere in hPa used in calculating the values. See Table 3 for the time intervals of the Low-Frequency Components. A comparison of the panels of Fig. 3 shows that the results referred to the three LOD_{atm} systems having the same top level of 10 hPa in the atmospheric general circulation model are similar in their low-frequency variations with time over the common intervals. Only at the beginning of the JMA interval, the JMA component is somewhat larger than that in the NCEP Reanalysis system. Compared to the ECMWF component, we notice in the bottom panel that the UKMO component varies less close over the same interval. This probably reflects that the top level in the atmosphere used in computing the wind term χ_3(W) of UKMO is only about 25 hPa. Concerning the significance of the Low-Frequency Components, we can say that the results in the NCEP Reanalysis, JMA and ECMWF systems with the same top level of 10 hPa are equivalent over the common interval. Therefore, in the following comparison with the LOD_{red} result, we will use only the NCEP Reanalysis component as the longest low-frequency series obtained from LOD_{atm}.

The Low-Frequency Components in the LOD_{red} and LOD_{atm} variations for the IERS and NCEP Reanalysis systems, respectively, are shown in Fig. 4. Compared to Fig. 3, the scale on the y-axis is smaller in the panels here, i. e., the resolution is now also smaller. In Fig. 4, the Low-Frequency Component of LOD_{red} is illustrated at the top and that of LOD_{atm} for the NCEP Reanalysis system at the centre. A comparison of the top panel of Fig. 3 with the middle panel of Fig. 4 shows that the Low-Frequency Component of LOD_{atm} in the NCEP Reanalysis system is different resolved in magnitude.

According to Section 3, the Low-Frequency Component filtered out from LOD_{atm} data for the wind term χ_3(W) is the El Niño-Southern Oscillation. Compared to that filtered out from LOD_{red} data, there is an obvious discrepancy

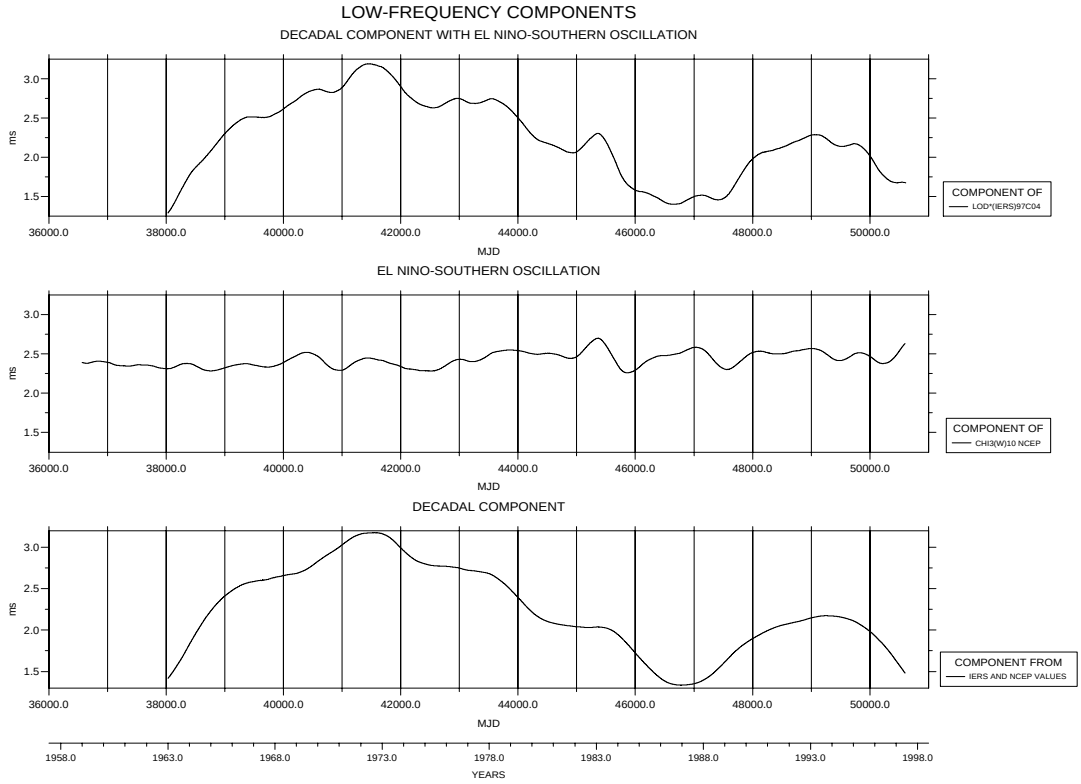

Figure 4. Low-Frequency Components in the LOD_{red} and LOD_{atm} variations for the IERS and NCEP Reanalysis systems, respectively. The Low-Frequency Component of LOD_{red} in the IERS system (top), that of LOD_{atm} in the NCEP Reanalysis system (centre) and the decadal component of LOD_{red} computed as difference series between the two Low-Frequency Components over the common interval (bottom).

between the results, which is shown by the curves in the top and middle panels of Fig. 4. As noted in Section 4, the explanation is that the Low-Frequency Component of LOD_{red} is composed of atmospheric and non-atmospheric contributions. We compute the non-atmospheric contribution over the common time interval as difference series between the Low-Frequency Component in the LOD_{red} variations for the IERS system (top of Fig. 4) and the Low-Frequency Component in the LOD_{atm} variations for the NCEP Reanalysis systems (centre of Fig. 4) removed the mean; see Table 3 for the intervals. The bottom panel of Fig. 4 shows the residual that is the decadal component of LOD_{red} for the IERS-NCEP Reanalysis system. The large, decadal-scale signal is thought to be caused primarily by core-mantle boundary processes (see Section 4).

(b) Quasi-Biennial Oscillation

Figure 5 presents the Quasi-Biennial Oscillations of the LOD_{atm} series in terms of the wind term χ_3(W) in the different systems. Similar to Fig. 3, the top panel gives the result in the NCEP Reanalysis system, the middle panel that in the JMA system and the bottom panel that in the UKMO system. As mentioned in Section 5.1, there is no QBO result for the ECMWF system due to a 10-month gap in the LOD_{atm} series produced operationally by the ECMWF. The time intervals of the QBO series are given in Table 3. As for the Low-Frequency Components, a comparison of the curves shows that the oscillations in the NCEP Reanalysis and JMA systems are in good agreement over the relatively short interval. The QBO component for the UKMO system is based on a top pressure level of about 25 hPa in computing the χ_3(W) values and therefore clearly disagrees with the results in the NCEP Reanalysis and JMA systems with 10 hPa top level over the common interval. The QBO results for the NCEP Reanalysis and JMA systems are of the same quality. However, for the lengthy of the time series resulting from the LOD_{atm} data for the NCEP Reanalysis system, we should restrict further investigations to the results in this LOD_{atm} system.

In Fig. 6, the Quasi-Biennial Oscillations in the LOD_{atm} variations for the NCEP Reanalysis system are shown, with the component of the wind term χ_3(W) plotted at the top, the components of the pressure term χ_3(P) and of the wind plus pressure term χ_3(W) + χ_3(P) at the centre and the components of the pressure IB term χ_3(P+IB) and of the wind plus pressure IB term χ_3(W) + χ_3(P+IB) at the bottom. A comparison of the results for χ_3(P) and χ_3(P+IB), respectively, with those for χ_3(W) shows that, in either case, the portion of the pressure term is too small (its amplitude is about 0.007 and 0.005 ms, respectively) to be significant for the total biennial signals. Therefore, the contributions of χ_3(P) and

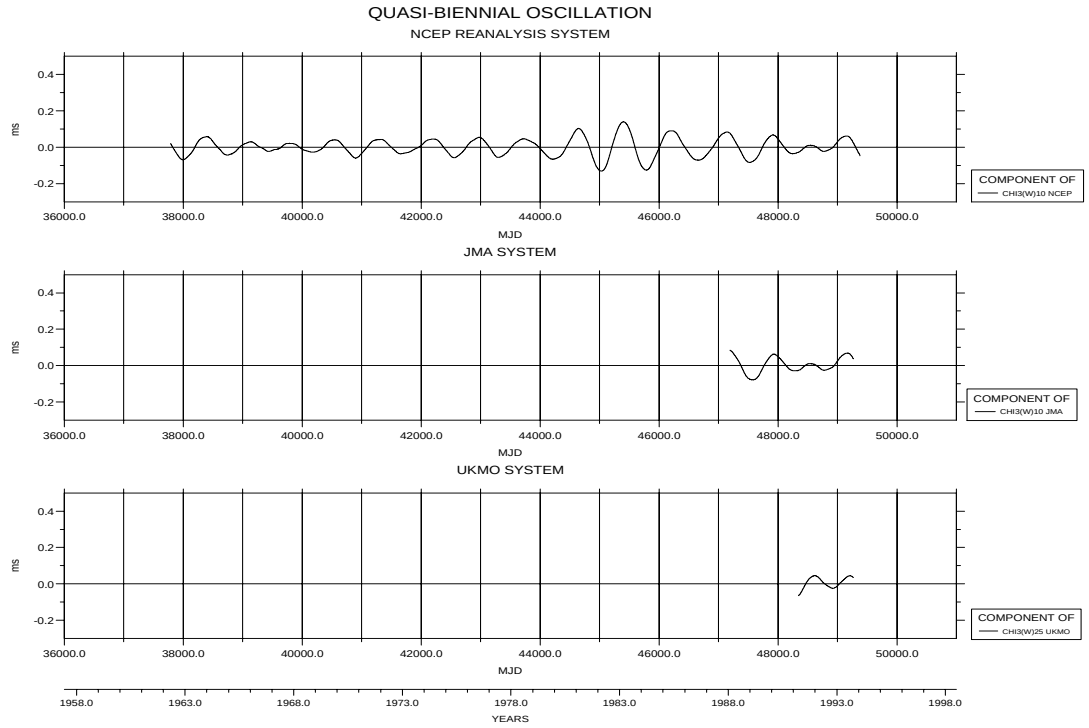

Figure 5. Quasi-Biennial Oscillations in the LOD_{atm} variations for the different systems: Oscillation of the wind term χ_3(W) in the NCEP Reanalysis system (top), in the JMA system (centre) and in the UKMO system (bottom). The number added to each χ_3(W) gives the upper pressure level in the atmosphere in hPa used in computing the values.

χ_3(P+IB) are ignored, and we refer to the QBO result as derived for the χ_3(W) term with 10 hPa top level of the NCEP Reanalysis system in the further discussion.

A comparison of the Quasi-Biennial Oscillation in the LOD_{atm} variations for the NCEP Reanalysis system with that in the LOD_{red} variations for the IERS system is shown in Fig. 7, with the top panel giving the results (A) obtained after band-pass filtering of the original data, the middle panel (B) as (A), but after removing the low-frequency and seasonal signals, and the bottom panel (C) as (B), but after using a band-pass filter of a broader bandwidth. Details about the two biennial filters used are given in Section 5.1. Generally, there is good agreement of both curves in each panel. However, comparing the resulting series obtained after different types of filtering, each plotted in another panel, we see that the amplitudes of the oscillations are different with time. In particular, the amplitude of (A) is considerably larger than that of (B) or (C). In assessing the results, the following should be noted:

Using the same filter applied to the original data and to the data after removing the low-frequency and seasonal oscillations, the biennial signal of (A) may be less attenuated than that of (B); the issue is not surprising. Therefore, the QBO series of (C) derived with a filter having a window width of only half compared to that of (A) and (B), should be more reliable than the results of (B). As can be seen in Fig. 7, the curves of (C) plotted at the bottom are more similar to those of (A) plotted at the top. But, in detail, there is some disagreement, which occurs when the variation is close to zero. Note that the curves referred to the NCEP Reanalysis and IERS systems of (A) with each other better coincide than those of (C) over the first third of the IERS interval. Obviously, the reason for this is that the uncertainty of the LOD_{red} series computed over different periods is still large; for the uncertainty see, e. g., IERS (1998). In view of the better agreement of the QBO series for (A), we regard these results as more significant than those for (C).

To facilitate a comparison of the QBO components obtained for the LOD_{red} and LOD_{atm} data and also the negative SOI data (see in (c) for using the negative of the data), the variability of their parameters with time is shown in Fig. 8. Here, the variations in amplitude are plotted at the top and those in period at the bottom. But, instead of the phase variability, the phase differences between LOD_{red} and LOD_{atm} and those between LOD_{atm} and SOI, computed at the maximum, zero crossing and minimum over the common intervals, are plotted at the centre. If the phase difference between LOD_{red} and LOD_{atm} is positive (negative), the LOD_{red} component is behind (ahead) of that of LOD_{atm}. Likewise, if the phase difference between LOD_{atm} and SOI is positive (negative), the LOD_{atm} curve is behind (ahead) of that of SOI. As can be seen, there is good agreement in the variability of the amplitude, phase and period of the QBO components of LOD_{red} and LOD_{atm}. Within the uncertainty (see Table 4), the oscillation at the quasi-biennial period, derived from the LOD_{red} variations in the IERS system, matches that derived from the LOD_{atm} variations, especially

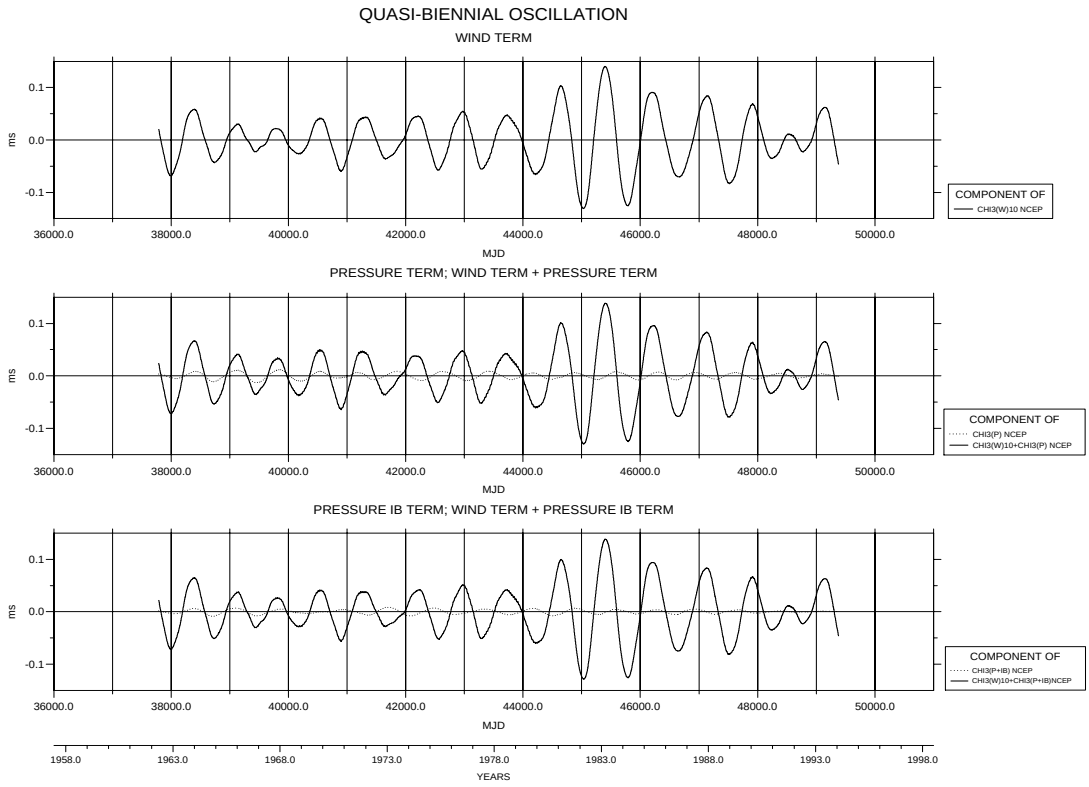

Figure 6. Quasi-Biennial Oscillations in the LOD_{atm} variations for the NCEP Reanalysis system: Oscillation of the wind term χ_3(W) (top), of the pressure term χ_3(P) and of the wind plus pressure term χ_3(W) + χ_3(P) (centre) and of the pressure IB term χ_3(P+IB) and of the wind plus pressure IB term χ_3(W) + χ_3(P+IB) (bottom). The number added to each χ_3(W) gives the upper pressure level in the atmosphere in hPa used in computing the values.

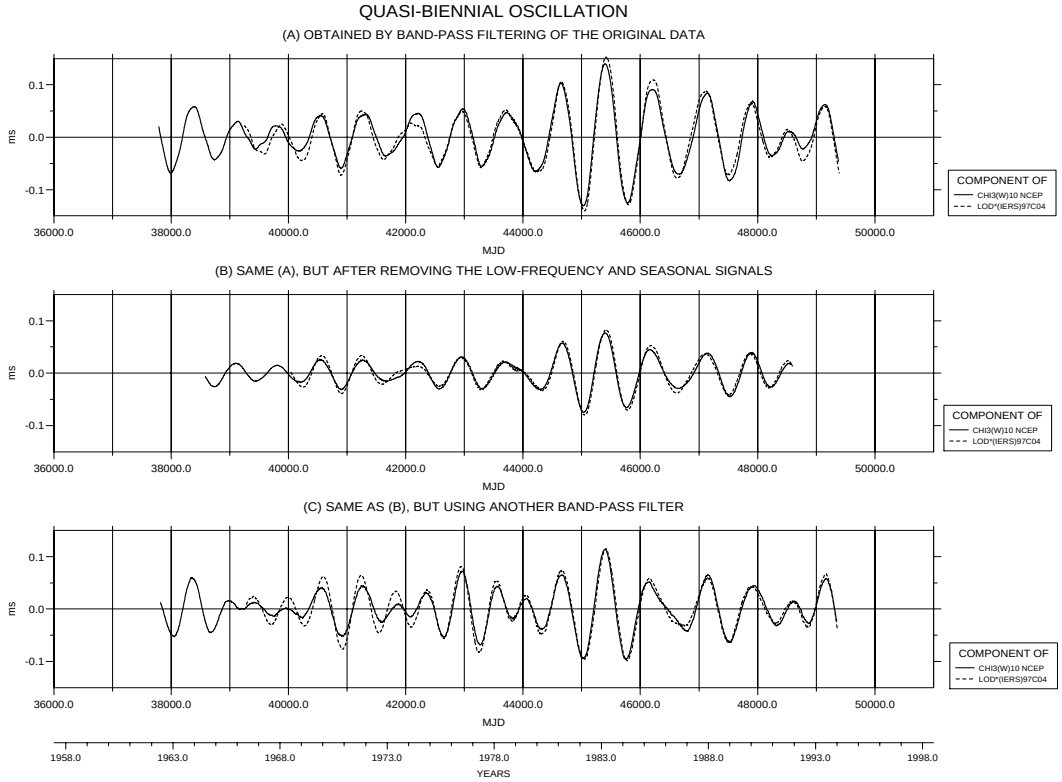

Figure 7. Comparison of the Quasi-Biennial Oscillations of LOD_{atm} in the NCEP Reanalysis system and of LOD_{red} in the IERS system: (A) obtained by band-pass filtering of the original data (top); (B) same as (A), but after removing the low-frequency and seasonal signals (centre); (C) same as (B), but using a band-pass filter of a broader bandwidth (bottom).

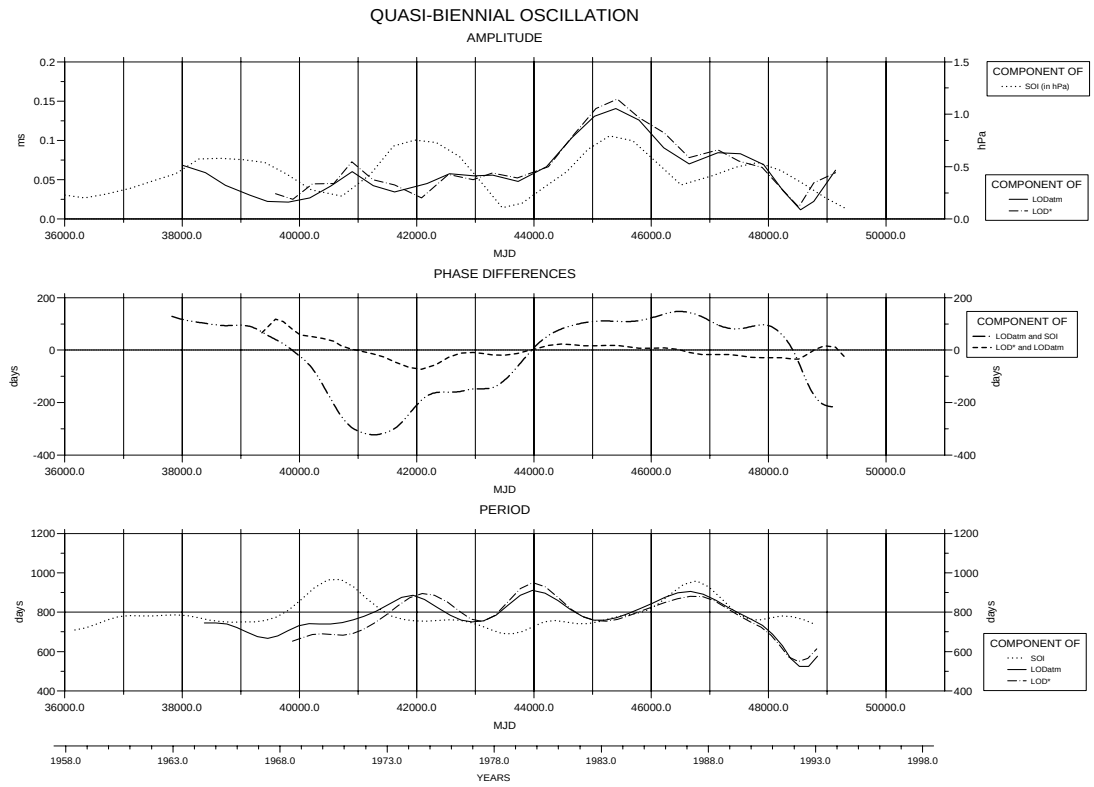

Figure 8. Parameter variability with time of the Quasi-Biennial Oscillations in LOD_{red}, LOD_{atm} and SOI: Amplitude variations (top), phase differences between LOD_{atm} and SOI as well as LOD_{atm} and LOD_{red} (centre) and period variations (bottom). For a positive (negative) phase difference, the first-mentioned component lags (leads) the second.

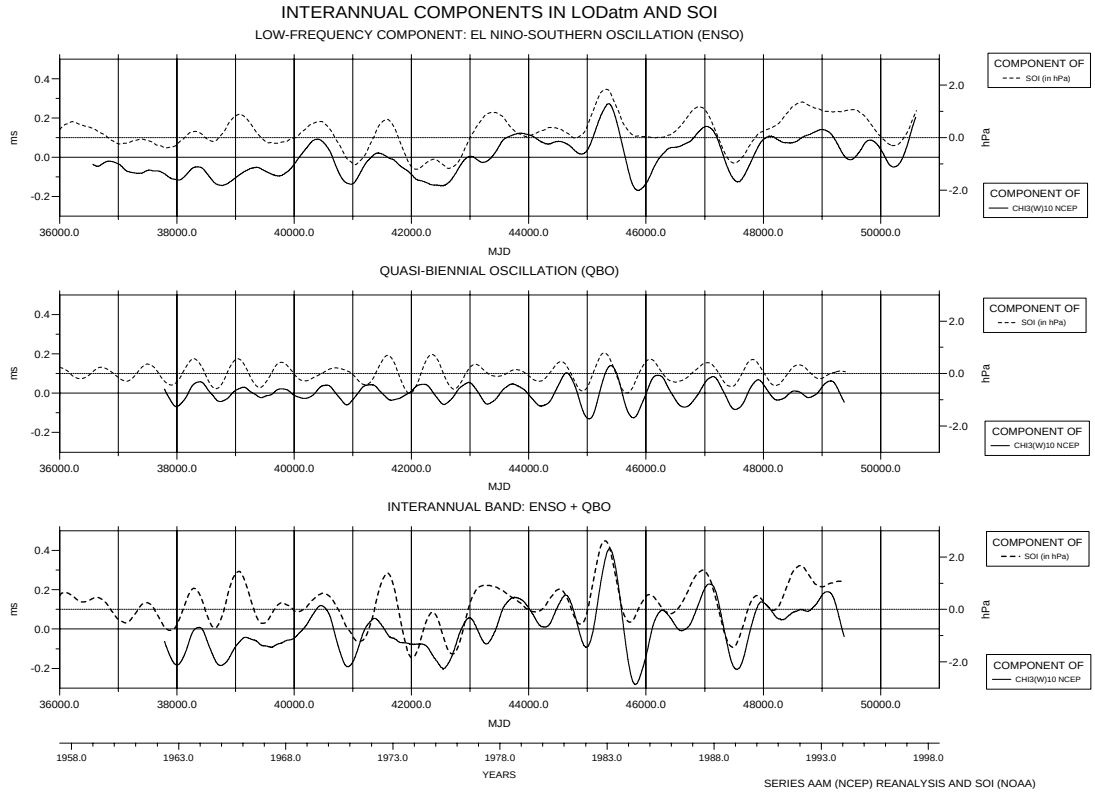

Figure 9. Interannual components of LOD_{atm} in the NCEP Reanalysis system and of the negative Southern Oscillation Index: El Niño-Southern Oscillation (top), Quasi-Biennial Oscillation (centre) and the interannual band (bottom).

for the χ_3(W) term with 10 hPa top level, in the NCEP Reanalysis system over the common interval, i. e., the solid Earth-atmosphere axial angular momentum budget for the quasi-biennial time scale is closed.

(c) Interannual components: ENSO, QBO and the interannual band

Figure 9 shows the interannual components of the LOD_{atm} series in the NCEP Reanalysis system as derived for the χ_3(W) term with 10 hPa top level (as solid curves, scale on left). Here, the El Niño-Southern Oscillation is plotted at the top (same as top of Fig. 3, but mean removed), the Quasi-Biennial Oscillation at the centre (same as top of Fig. 5), and the interannual band, incorporating both components over the common interval, at the bottom. Also shown in each panel is the corresponding component of the negative Southern Oscillation Index (as dashed curves, scale on right). Concerning the ENSO cycles including El Niño and La Niña events as extreme phases, the full interannual LOD_{atm} and SOI variations with time should reflect these climate changes (see Section 3). If there is a negative SOI number, we have an El Niño, i. e., warming of the surface of the central and eastern Pacific, but if the SOI number is positive, we have a La Niña, i. e., ocean cooling. Note that the components of the negative SOI are plotted in a way that the curves are parallel with those of the LOD_{atm} series. The curves clearly exhibit the characteristics and the time evolution of the signals that we shall discuss in detail.

For the ENSO component of the LOD_{atm} variations in the NCEP Reanalysis system, we obtained the highest positive amplitude estimate of 0.273 ms in February 1983 (MJD 45373.0) and the lowest negative estimate of 0.169 ms during June/July 1984 (MJD 45881.0). In Table 4, the ranges of the variations in amplitude, separately for positive and negative estimates, and period for the Quasi-Biennial Oscillation in LOD_{red}, LOD_{atm} for the NCEP Reanalysis system, as derived for the χ_3(W) term with 10 hPa top level, and in SOI are compiled for comparison. Also, the standard errors of the estimates and the means as computed from double measurements are included. For details of their calculation, see Höpfner (1997).

Concerning the total interannual LOD_{atm} variations, the extreme amplitude estimates reach +0.410 and -0.282 ms in February 1983 (MJD 45377.0) and April 1984 (MJD 45817.0), respectively. In the case of SOI, there are the following extreme estimates: +1.842 hPa in December 1982 (MJD 45317.9) and -1.206 hPa in January 1974 (MJD 42061.3) for the ENSO component and +2.609 hPa in December 1982 (MJD 45317.9) and -1.848 hPa in November 1973 (MJD 42000.4) for the total signal.

At the interannual time scale, the ENSO component referred to the LOD_{atm} system varies in both amplitude and

Table 4. Ranges of the variations of the Quasi-Biennial Oscillation in amplitude and period including the standard errors of the estimates. Min, minimum; Max, maximum; Dif, difference between maximum and minimum; s_0, standard error of a single estimate; $s_{amplitude}$, standard error of an amplitude mean; s_{period}, standard error of a period three-point mean; n, number of pairs; in case of the period, number of differences.

Amplitude estimates (ms; in case of SOI, hPa)

Time series	Ranges of the variations			Standard deviation		
	Min	Max	Dif	s_0	$s_{amplitude}$	n
LOD_{red}	0.015	0.153	0.138	0.012	0.009	13
	-0.032	-0.141	-0.109			
LOD_{atm}: NCEP Reanalysis	0.012	0.140	0.128	0.014	0.010	15
	-0.022	-0.131	-0.109			
SOI	0.109	0.754	0.645	0.090	0.064	18
	-0.093	-0.792	-0.699			

Period estimates (days)

Time series	Ranges of the variations			Standard deviation		
	Min	Max	Dif	s_0	s_{period}	n
LOD_{red}	548.1	952.0	403.9	34.1	19.7	24
LOD_{atm}: NCEP Reanalysis	524.8	912.2	387.4	34.6	20.0	28
SOI	688.1	969.0	280.9	28.1	16.2	34

duration with time considerably, while the QBO component is essentially stationary (compare the upper panel with the middle panel in Fig. 9). The total interannual signal obtained after superposing the two components either constructively or destructively is shown in the bottom panel. Compared to it, the corresponding SOI components are rather similar in their time dependence, except for some intervals with mostly weak signals. Since the LOD_{atm} and LOD_{red} data are global quantities, while the SOI series is derived from local measurements, no perfect similarity between the LOD_{atm} and SOI components can be expected.

For the ENSO component, a disagreement between the LOD_{atm} and SOI series from their beginning to 1968 exists, since the LOD_{atm} estimates are always lower-negative. Another disagreement indicated by negative values can be seen in 1984. The QBO component is displayed in Figs. 8 and 9. The top panel of Fig. 8 shows that the courses of the resulting QBO series of LOD_{atm} and SOI differ in magnitude during 1972-1974, i. e., the LOD_{atm} amplitude estimates are relatively large. Moreover, as presented in the middle panel of Fig. 8, there is considerable variability in the phase difference. The year 1962 shows positive values, becoming gradually smaller and approaching zero in 1968. After that, the values are negative. After 1971, they become smaller and again approach zero in 1979. During the interval from 1979 to 1991, the values are positive values and, after that, again negative. As noted above, if the phase difference between LOD_{atm} and SOI is positive (negative), the LOD_{atm} curve is behind (ahead) of that for SOI. Comparing the variations in period of LOD_{atm} and SOI, shown in the bottom panel of Fig. 8, we notice that both curves differ considerably from the beginning of the common interval to 1980, while there is good agreement after this until 1991. Afterwards, the period variabilities of the LOD_{atm} and SOI components are again less conformable with time. The comparison suggests that, if the QBO signals are of pronounced magnitude, the variations in SOI are followed by changes in LOD_{atm} about 120 days later, where the average period is about 800 days. The wavelet time-frequency spectra of the LOD excess and of the AAM (JMA) for the wind term computed from 1976 to 1994 and from 1984 to 1994, respectively, by Chao and Naito (1995) are used for a comparison with the QBO curves referred to the IERS and NCEP Reanalysis systems, respectively, illustrated here. Concerning magnitude and temporal behaviour, the results coincide with each other.

Finally, we discuss and assess the total interannual signals of LOD_{atm} and SOI plotted in the bottom panel of Fig. 9. As can be seen, there is considerable variability in the ENSO cycle during the decades. For example, the 1970's are characterized by a relatively inactive cycle, whereas in the 1980's and 1990's the cycle was quite pronounced. As mentioned above, the total ENSO signature results from interaction between the distinct Low-Frequency and Quasi-Biennial components. Constructive interference of the Low-Frequency component and the QBO component results in an intense event. Conversely, mild events are associated with destructive interference of these components. Comparison of the three panels of Fig. 9 shows that the positive and negative modulations are visible as extremes. Here, maxima being mostly positive indicate El Niño events and minima being mostly negative La Niña events. There are, for example, the big El Niño event in 1982/83 and the strong La Niña event in 1988/89, for which both components are in phase with positive and negative polarities, respectively, and full constructive interference occurs. In Table 5, the extremes of the total interannual signals of SOI that suggest El Niño and La Niña events in the ENSO cycle are summarized with those of LOD_{atm}. Moreover, the lag values, each computed as phase difference between the epochs of the corresponding SOI and LOD_{atm} extremes in days, are listed. Here, a positive difference indicates that the LOD_{atm} extreme follows that

Table 5. Extremes suggesting El Niño and La Niña events in the ENSO cycle. A positive phase difference indicates that the LOD_{atm} extreme follows that of SOI. Its standard error, i. e. standard error of a single estimate, is about $\pm$43 days.

Year(s)	Accepted event	MJD	SOI extreme (hPa)	MJD	LOD_{atm} extreme (ms)	Date	Phase difference (days)
		35548.02	-1.196			(March 1956)	
1957	El Niño	36095.87	0.659			(Sept. 1957)	
		37130.69	-0.511			(July 1960)	
		37495.92	0.252			(July 1961)	
1962	La Niña	37922.02	-0.799	38007.00	-.183	Dec. 1962	85
1963	El Niño	38287.25	0.804	38383.00	0.009	Dec. 1963	96
		38652.48	-0.709	38737.00	-.186	Dec. 1964	84
1965	El Niño	39048.14	1.454	39181.00	-.041	Feb. 1966	133
1967	La Niña	39474.25	-0.535	39605.00	-.093	April 1967	131
		39778.61	0.259			(Oct. 1967)	
		40052.53	-0.102			(July 1968)	
1969	El Niño	40478.63	0.615	40451.00	0.120	Aug. 1969	-28
1970/71	La Niña	41117.79	-1.219	40926.00	-.191	June 1971	-192
1972	El Niño	41604.76	1.387	41365.00	0.055	Feb. 1972	-240
1974/75	La Niña	42000.42	-1.848			(Nov. 1973)	
		42365.65	-0.108			(Nov. 1974)	
		42700.45	-1.703	42541.00	-.203	Oct. 1975	-159
1976/77	El Niño	43248.29	0.937	42979.00	0.059	April 1977	-269
				43278.00	-.076	(May 1977)	
				43757.00	0.163	(Sept. 1978)	
		44130.93	-0.099	44248.00	0.009	Jan. 1980	117
		44526.60	0.778	44645.00	0.173	Feb. 1981	118
		44891.83	-0.563	44976.00	-.093	Jan. 1982	84
1982/83	El Niño	45317.93	2.609	45377.00	0.410	Feb. 1983	59
1984/85	La Niña	45713.60	-0.484	45817.00	-.282	April 1984	103
		46048.39	0.563	46282.00	0.097	Aug. 1985	234
	La Niña	46413.62	-0.175	46577.00	-.007	May 1986	163
1986/87	El Niño	46961.47	1.498	47076.00	0.229	Oct. 1987	115
1988/89	La Niña	47478.88	-1.458	47527.00	-.204	Jan. 1989	47
		47874.54	0.526	47973.00	0.139	March 1990	98
		48148.46	-0.036	48272.00	0.050	Jan. 1991	124
1991-93	El Niño	48635.44	1.676			(Jan. 1992)	
		49000.67	0.857	49078.00	0.190	March 1993	77

of SOI; the standard error of the estimates is $\pm$43 days. Except for the decade in which the ENSO cycle was inactive, we find that the El Niño- and La Niña-related signals in SOI are followed by those in LOD_{atm} with a lag of about (110$\pm$10) days, which is similar to that for the QBO component. It should be noted that the variations obtained from the SOI series from 1976 to 1991 by Dickey, Marcus and Hide (1992) for a low-frequency band between 32 and 88 months, for a quasi-biennial band between 18 and 35 months and for an interannual band between 18 and 88 months agree well with our SOI results plotted in the three panels of Fig. 9. However, the lead of SOI with respect to the interannual LOD is different in previous studies. For example, Chao (1984) reported that the SOI leads the interannual LOD by 1 month during 1957-1983, while Eubanks et al. (1986) and Chao (1988) reported a lead time of 3 months during 1962-1985 and of 2 months during 1972-1986, respectively.

7 Summary and concluding remarks

The variability in the Earth's climate system is considerable on a number of time and space scales. The longer time-scale phenomena are usually associated with changes in the atmospheric and oceanic circulation over large portions of one hemisphere or even the whole globe. These modifications of the circulation result in abnormal temperature, rainfall and other weather patterns. In general, it is observed that the longer the significant time-scale of the phenomena, the larger the space-scale of the features. On the interannual time scale, there are significant fluctuations that include the El Niño-Southern Oscillation (ENSO) and the Quasi-Biennial Oscillation (QBO). Fluctuations in the axial component χ_3 of the Atmospheric-Angular-Momentum (AAM) and in the Length-Of-Day (LOD) on this time scale are attributed to

changes in the Earth's climate system associated with changes in the strength of motion fields and redistributions of mass. After studying the imbalances in the solid Earth-atmosphere axial angular momentum budget on the seasonal time scale, published in our previous papers (Höpfner, 1996, 1997,1998a, b), the present investigation focusses on the interannual fluctuations in LOD and LOD_{atm}. Here, LOD_{atm} is the atmospheric contribution to LOD inferred from AAM.

To quantify the Low-Frequency Component and the Quasi-Biennial Oscillation in LOD and LOD_{atm} in their temporal variability, the following time series with one-day sampling are used:

(a) LOD of the series EOP (IERS) 97C04 from 1962 to 1998;

(b) LOD_{atm} in terms of χ_3 of the series AAM (NCEP) Reanalysis from 1958 to 1998, AAM (JMA) from 1983 to 1998, AAM (ECMWF) from 1988 to 1996 and AAM (UKMO) from 1986 to 1998.

Here, the χ_3 component comprises the wind term χ_3(W) and the pressure term χ_3(P) or the pressure term with Inverted-Barometer response χ_3(P+IB). The top pressure level in the general circulation models of the meteorological centers used for calculating the wind terms is 10 hPa in the NCEP Reanalysis, JMA and ECMWF models and about 25 hPa in the UKMO model.

Since the LOD data in the IERS system still include all oscillations due to zonal tides, these periodic components are removed according to IERS conventions. Therefore, after removing the tidal contribution, LOD_{red} stands for LOD. To make the operational LOD_{atm} series in the JMA, ECMWF and UKMO systems free of gaps and discontinuities, like in the previous studies, the pre-processing of these time series is completed and carried out, respectively. For comparison, we also process the monthly Southern Oscillation Index (SOI) time series, as computed and standardized by NOAA, in the same manner as the LOD_{red} and LOD_{atm} time series.

To separate the interannual signals, in particular the Low-Frequency Component and the Quasi-Biennial Oscillation, from the original LOD_{red} series and from the different LOD_{atm} series with one-day sampling, we apply a low-pass filter and a biennial band-pass filter, each designed as a zero-phase digital filter. But, because of a data gap of 10 months, no QBO component could be filtered out from the LOD_{atm} series in the ECMWF system. For purposes of comparison, after removing the low-frequency and seasonal signals from the LOD_{red} and LOD_{atm} time series, the QBO component is also computed. Here, two biennial filters are used, namely that already mentioned and a filter of a broader bandwidth. Using a simple method described in previous papers (Höpfner, 1997, 1998b), optimal estimates of the amplitude and period of the Quasi-Biennial Oscillation, including the standard deviations, are computed. For separating the Low-Frequency Component and the Quasi-Biennial Oscillation from monthly values, we design zero-phase digital low-pass and biennial filters. Both are applied to process the monthly SOI time series. Optimal estimates of the amplitude and period for the resulting QBO component and their standard errors are calculated in a similar manner as noted above.

Comparing the results derived from the LOD_{red} series, the different LOD_{atm} series and the SOI series for low-frequency and biennial time scales, we discuss the characteristics of the Low-Frequency Component, the Quasi-Biennial Oscillation and the total interannual signal. The main results are the following:

The Low-Frequency Components in the LOD_{atm} data, especially for the wind term χ_3(W) in the NCEP Reanalysis, JMA, and ECMWF systems with the same top pressure level of 10 hPa, referred to as El Niño-Southern Oscillations, are similar in their variations with time over the common interval, i. e. to assess as equivalent results. Therefore, for a comparison with the LOD_{red} component in the IERS system, we use only the NCEP Reanalysis component as the longest LOD_{atm} series obtained on the low-frequency time scale. There is a distinct discrepancy between both time series. The reason for this is that the LOD_{red} component comprises atmospheric and non-atmospheric portions. As difference series between the Low-Frequency Component in the LOD_{red} variations of the IERS system and the Low-Frequency Component in the LOD_{atm} variations in the NCEP Reanalysis system, after removing the mean, we compute the non-atmospheric signal at one-day intervals over the common interval. It is defined to be the decadal LOD_{red} component referred to the IERS-NCEP Reanalysis system and probably caused primarily by core-mantle boundary processes.

The Quasi-Biennial Oscillations in the LOD_{atm} variations, again for the χ_3(W) terms having the same top level of 10 hPa, of the NCEP reanalysis and JMA systems agree well over the short common interval. To produce a significant effect, the quasi-biennial signals of the pressure terms χ_3(P) and χ_3(P+IB), respectively, i. e. without and with IB response, are too small, when included in the quasi-biennial χ_3(W) oscillation. Comparing the QBO results filtered out from LOD_{atm} data for the χ_3(W) term in the NCEP Reanalysis system and LOD_{red} data in the IERS system in several ways, including (A) band-pass filtering of the original data, (B) same as (A), but after removing the low-frequency and seasonal signals, and (C) same as (B), but using a band-pass filter of a broader bandwidth, there is good agreement between both components after the same way, but disagreement between them after different ways. For some reason, we regard the results for (A) as more significant as the results for (B) and (C). In a similar manner, the QBO signals of the LOD_{atm} data in the NCEP Reanalysis system and of the LOD_{red} data in the IERS system vary in amplitude, phase and period within their uncertainties, i. e., on the quasi-biennial time scale, a balance exists in the solid Earth-atmosphere axial angular momentum budget. When the magnitude is large, the QBO component of SOI leads that of LOD_{atm} by about 100 days.

In the LOD_{atm} variations referred to the NCEP Reanalysis system, the ENSO and the QBO components are very

dissimilar: The variability with time in amplitude and duration of the ENSO signal is considerable. Here, the highest positive amplitude is 0.273 ms for the El Niño event in 1982/83, and the lowest negative amplitude is 0.169 ms for the La Niña event in 1984/85. Over the entire ENSO interval, there exist a first large variation with a peak-to-peak amplitude of about 0.23 ms between 1969 and 1971 and several large variations after 1983. On the contrary, the QBO signal is essentially stationary. It has an amplitude between -0.131 ms and +0.140 ms and a period between 650 and 900 days, except after 1991 when the period is less than 550 days. Both components constitute the total interannual signal, and show when ENSO events occur. Intense El Niño (La Niña) events require constructive interference at positive (negative) polarity, whereas mild events result from destructive interference. In case of SOI, we use the negative of the SOI data to be in parallel with the time evolution of the LOD_{atm} data. In the ENSO cycle, there is considerable variability over the decades. The 1970's are characterized by a relatively inactive cycle, while the 1980's and 1990's feature quite pronounced cycles. A comparison of the total El Niño- and La Niña-related signals in the LOD_{atm} and SOI variations shows that their evolutions are similar during decades with active ENSO cycle. However, the interannual SOI signal leads that of LOD_{atm} by 110 days.

For the interannual time scale, the main results of the paper are quantitative estimates of the Low-Frequency Component and the Quasi-Biennial Oscillation in the LOD_{red}, LOD_{atm} and SOI variations and quantitative estimates of the total LOD_{atm} and SOI signals in their temporal variability. Furthermore, the decadal LOD_{red} component is available as a function of time. The results show the character and the time evolution of the various contributions, which should help interpreting the interannual LOD changes associated with such climate phenomena as the global-scale ENSO cycles. Compared with previous studies, it should be noted that this study is based on the full AAM (NCEP) Reanalysis series.

Acknowledgement. Some results of this paper were presented during the Geodetic Week at the University of Kaiserslautern, Germany, in October 1998 and published in German (Höpfner, 1998c). I would like to thank Dr Detlef Wolf for his linguistic advice that helped to improve the quality of this paper.

References

Barnes, R. T. H., Hide, R., White, A. A. and Wilson, C. A., 1983. Atmospheric angular momentum fluctuations, length-of-day changes and polar motion, *Proc. Roy. Soc. Lond., A, 387*, 31–73.

Chao, B. F., 1984. Interannual length-of-day variations with relation to the Southern Oscillation/El Niño, *Geophys. Res. Lett., 11*, 541–544.

Chao, B. F., 1988. Correlation of interannual length-of-day variation with El Niño/Southern Oscillation, *J. Geophys. Res., 93*, 7709–7715.

Chao, B. F., 1989. Length-of-day variations caused by El Niño-Southern Oscillation and Quasi-Biennial Oscillation, *Science, 243*, 923–925.

Chao, B. F. and Naito, I., 1995. Wavelet analysis provides a new tool for studying Earth's rotation, *EOS, Transactions, AGU, 76*, 16, p. 161, 164–165.

Dickey, J. O., 1990. Atmospheric Excitation of the Earth's rotation. In: Boucher, C. and Wilkins, G. A. (Eds.), *Earth Rotation and Coordinate Reference Frames*. Springer-Verlag, 58–66.

Dickey, J. O., Marcus, S. L. and Hide, R., 1992. Global propagation of interannual fluctuations in atmospheric angular momentum, *Nature, 357*, 485–488.

Dickey, J. O., Marcus, S. L., Hide, R., Eubanks, T. N. and Boggs, D. H., 1994. Angular momentum exchange among the solid Earth, atmospheres and oceans: A case study of the 1982-1983 El Niño event. *J. Geophys. Res., 99*, 23921–23937.

Eubanks, T. M., Steppe, J. A. and Dickey, J. O., 1986. The El Niño, the Southern Oscillation and the Earth rotation. In: *Earth Rotation: Solved and Unsolved Problems*, edited by A. Cazenave. D. Reidel, Dordrecht, Holland, 163–186.

Gross, R. S., Marcus, S. L., Eubanks, T. M., Dickey, J. O. and Keppene, C. L., 1996. Detection of an ENSO signal in seasonal length-of-day variations, *Geophys. Res. Lett., 23*, 3373–3376.

Hide, R. and Dickey, J. O., 1991. Earth's variable rotation, *Science, 253*, 629–637.

Höpfner, J., 1996. Seasonal oscillations in length-of-day, *Astron. Nachr., 317*, 273–280.

Höpfner, J., 1997. *Seasonal variations in length-of-day and atmospheric-angular-momentum*, Scientific Technical Report STR97/08, GeoForschungsZentrum Potsdam.

Höpfner, J., 1998a. *Seasonal length-of-day changes and atmospheric-angular-momentum oscillations in their temporal variability*, Scientific Technical Report STR98/10, GeoForschungsZentrum Potsdam.

Höpfner, J., 1998b. Seasonal variations in length-of-day and atmospheric-angular-momentum, *GJI, 135*, 407–437.

Höpfner, J., 1998c. Variationen in der Tageslänge und dem atmosphärischen Drehimpuls im Zeitbereich von einigen Jahren. In: *Progress in Geodetic Science at GW 98*. Edited by Willi Freeden. Shaker Verlag, Aachen, 106–113.

IERS, 1998. *1997 IERS Annual Report*, Central Bureau of IERS. Observatoire de Paris.

Jochmann, H. and Greiner-Mai, H., 1996. Climate variations and the Earth's rotation, *J. Geodynamics, 21*, 161–176.

Kalnay, E., Kanamitsu, M., Kistler, R. et al., 1996. The NCEP/NCAR 40-year reanalysis, *Bull. Amer. Meteor. Soc., 77*, 437–471.

McCarthy, D. D. (ed.), 1996. *IERS Conventions (1996)*, IERS Technical Note 21. Central Bureau of IERS. Observatoire de Paris.

Nuzhdina, M., Kołaczek, B. and Kosek, W., 1997. *Influence of ENSO on correlations between seasonal and subseasonal variations of Earth rotation and atmospheric angular momentum*, Paper presented at the XXII General Assembly of the European Geophysical Society. Vienna, Austria, 21-25 April 1997.

Peixoto, J. P. and Oort, A. H., 1992. *Physics of climate*, American Institute of Physics, New York.

Rosen, R. D., 1993. The axial momentum balance of Earth and its fluid envelope, *Surveys in Geophysics, 14*, 1–29.

Salstein, D. A. and Rosen, R. D., 1986. Earth rotation as a proxy for interannual variability in atmospheric circulation, 1860-present, *J. Clim. Appl. Meteorol., 25*, 1870–1877.

Salstein, D. A. and Rosen, R. D., 1997. Global momentum and energy signals from reanalysis systems, Reprint volume. *7th Conference on Global Climate Variations*. American Meteorological Society, 344–348.

Salstein, D. A. and Rosen, R. D., 1998. Interannual signals in atmospheric angular momentum from a 40 year reanalysis, *Annales Geophysicae, 16, Suppl. I*, C386. Paper presented at the XXIII General Assembly of the European Geophysical Society. Nice, France, in April 1998.

Salstein, D. A., Kann, D. M., Miller, A. J. and Rosen, R. D., 1993. The Sub-bureau for Atmospheric Angular Momentum of the International Earth Rotation Service: A Meteorological Data Center with Geodetic Applications, *Bull. Amer. Meteorol. Soc., 74*, 67–80.